Journal of Southeast University (English Edition) Vol. 33, No. 3, pp. 293 - 300 Sept. 2017 ISSN 1003—7985

Simulation of meso factors influencing fracture performance of dense-graded asphalt concrete at low temperature

Zhang Yao[1] Huang Xiaoming[1] Ma Tao[1] Zhang Deyu[2]

([1]School of Transportation, Southeast University, Nanjing 210096, China)

([2]School of Architecture Engineering, Nanjing Institute of Technology, Nanjing 211167, China)

Abstract: In order to characterize the impacts of key factors on the low-temperature fracture performance of dense-graded asphalt concrete, the virtual bending fracture test is simulated by using the discrete element method (DEM) and emulation software PFC3D (particle flow code in three-dimension). A virtual specimen generation procedure consisting of aggregate gradation, irregular clumps, asphalt mortar and air void content is performed based on the random generation algorithm and irregular coarse aggregates library. Then, the virtual fracture test is conducted after adding the micro mechanical contact models to the specimen, and the validity of virtual modeling is verified by the comparison of simulation test data and lab test data. Additionally, an orthogonal test is designed to investigate the impacts of the volume fraction of coarse aggregates and air voids, stiffness of coarse aggregates and asphalt mortar, internal bond strength of asphalt mortar and distribution of coarse aggregates and air voids on low-temperature fracture performance based on virtual simulation. The results show that all the factors have effects on fracture performance to various degrees, while the value of the bond strength of asphalt mortar is found to be the most important determinant of tensile strength and strain-energy density. The volume fraction of coarse aggregates is considered to be the most important determinant of tensile strain. Therefore, to obtain a high low-temperature fracture performance of dense-graded asphalt concrete, it is important to consider the microstructure and properties of asphalt mortar and aggregates.

Key words: asphalt mixture; fracture property; low temperature; virtual test; PFC3D; influence factors

DOI: 10.3969/j.issn.1003-7985.2017.03.007

Cracking is one of the main premature pavement risks particularly in cold winter, and various types of cracks are created at a low temperature when the thermal stress induced exceeds the tensile strength of the asphalt concrete pavement. Although laboratory tests in this field have been carried out for years, present knowledge is insufficient to fully evaluate the influences of different constituents and their distributions on asphalt concrete as a typical heterogeneous composite material[1-2]. Laboratory test results affected by the limitation of test conditions usually exhibit more variability, and results may be different in parallel specimens with the same aggregates grade and material composition. The main reason is that the variability of aggregate crushing and air voids distribution cannot be controlled by a laboratory test. Consequently, current specifications and laboratory test procedures do not adequately prevent low-temperature cracking of asphalt pavements. Numerous studies proved that the mechanical properties of asphalt mixture are significantly influenced by meso structures and material properties[3-5]. Therefore, it is necessary to introduce the meso-mechanical analysis method, a more precise analysis method, to investigate the fracture mechanism of asphalt mixture.

In recent years, the discrete element method with the advantages of analysis of meso-mechanical characteristics of heterogeneous materials has attracted much attention of many road and geotechnical researchers making the meso-mechanics simulation method more widely used. Numerical simulation methods are applied to investigate the fracture behavior and anti-crack characteristics of asphalt mixture. Wagoner et al.[6-7] used a single edge notched beam test and disk-shaped compact tension test to simulate fracture behavior and obtained the fracture energy of asphalt mixture. Based on the discrete element method, Kim et al.[8] simulated the cantilever beam test to compare the difference between using the continuous elastic theory and the discontinuous theory, and the bilinear cohesive zone model was used to observe the crack initiation and propagation. Based on the digital image processing technology, Kim et al.[9] built a two-dimensional discrete element model of asphalt mixture to investigate the indirect tensile heterogeneous fracture behavior, and used the user-defined energy-based bilinear cohesive zone model to simulate the crack initiation and propagation of the asphalt mixture specimen. Chen et al.[10] used a user-defined parametric model to investigate the virtual splitting behavior of the asphalt mixture at -10 and 15 ℃, and studied the porosity and aggregate volume fraction impact on the virtual splitting test results. Mahmoud et al.[11] presented a synthetic

Received 2016-11-18.

Biographies: Zhang Yao (1992—), female, graduate; Huang Xiaoming (corresponding author), male, doctor, professor, huangxm@seu.edu.cn.

Foundation item: The National Natural Science Foundation of China (No. 51378006, 51378121).

Citation: Zhang Yao, Huang Xiaoming, Ma Tao, et al. Simulation of meso factors influencing fracture performance of dense-graded asphalt concrete at low temperature[J]. Journal of Southeast University (English Edition), 2017, 33(3): 293 - 300. DOI: 10.3969/j.issn.1003-7985.2017.03.007.

method with image processing and discrete element combination to simulate the anti-cracking property of hot asphalt mixture. The result shows that the elastic model is useful for predicting the time-independent property of asphalt binder. Wang et al. [12] proposed a randomly-truncating algorithm to simulate the three-dimensional fracture behavior of epoxy asphalt mixture, and applied the bilinear displacement-softening model to simulate crack initiation and propagation. Based on DEM, Eckwright et al. [13] simulated the crack behavior with a single edge notched beam and semi-circular notched beam of asphalt mixture, respectively. Yang et al. [14] simulated single edge notched beam tests by using the discrete particle model, and after doing induction healing by raised temperature, the fracture strength recovery ratio was measured by the secondary loading. Chen et al. [15] used a user-defined three-dimensional parametric model to investigate three-point bending fracture behavior at −10 and 15 ℃, and discussed the influence of the cohesive and adhesive force of asphalt mortar on fracture test results. However, there is no systematic analysis of the impact of meso-scale factors on fracture performance.

Therefore, in order to systematically study the effect of meso-material composition and mechanical characteristics of asphalt mixture on bending fracture behavior at a low temperature, this study focuses on the analysis of how meso-scale factors affect bending fracture test results by using three-dimensional discrete element simulation. First, "Fish" code is used to generate a three-dimensional specimen of the asphalt mixture and to select an appropriate meso-mechanical contact model for the virtual bending test, where mechanical parameters can be obtained from bending tests and static uniaxial creep tests. Then, equivalent conditions are set to perform virtual tests, and virtual test results are compared with laboratory test results to validate the effectiveness of the simulation. Secondly, the orthogonal design process is used to analyze the influence of meso-scale factors on bending fracture test results. Macro factors including aggregates grading, asphalt-aggregate ratio and air voids are transformed into meso-scale factors of volume fractions of particulate material, while rock type, angularity, and viscosity of asphalt are converted into aggregate stiffness, friction coefficient and the bond strength of asphalt mortar, respectively.

1 Laboratory Test

1.1 Material gradation

A dense-graded asphalt concrete (AC-13) with nominal maximum aggregate size of 13.2 mm is used for the bending fracture test by Universal Testing Machine (UTM). The gradation of AC-13 and asphalt mortar (including asphalt, fillers and fine aggregates with the maximum size of 2.36 mm) are shown in Tab. 1 and Tab. 2, respectively.

Tab. 1 Gradation of AC-13

Sieving size/mm	16	13.2	9.5	4.75	2.36	1.18	0.6	0.3	0.15	0.075
Passing ratio/%	100	95	79.7	49.8	37.6	26.4	17.1	9.8	7.2	6.6

Note: Asphalt content is 5.1%.

Tab. 2 Gradation of asphalt mortar

Sieving size/mm	2.36	1.18	0.6	0.3	0.15	0.075
Passing ratio/%	100	70.2	45.4	26.1	19.1	17.6

Note: Asphalt dosage is 11.1%.

1.2 Experimental tests

The uniaxial compression test of asphalt mortar is performed on a cylinder sample by UTM to obtain a stress-strain curve with a compression strain rate of 0.008 3 s^{-1}, as shown in Fig. 1, and the slope of the linear fitting curve represents the macro elastic modulus of asphalt mortar, which is 2 439 MPa.

The three-point bending test is applied for the laboratory tests and micromechanical modeling, as shown in Fig. 2. The specimen size is set to be 250 mm × 30 mm × 35 mm. The load rate is set to be 50 mm/min and the test temperature is −10 ℃. Load span and load width are set to be 200 mm and 10 mm, respectively.

The damage process in the fracture test of the asphalt mixture at a low temperature is regarded as energy dissipation, and the work done by the external force on the material can be converted into strain energy storage. The critical value of strain-energy density is considered to be the area under the actual single strain-stress relationship curve end at the fracture point. It can be expressed as

$$\frac{d_w}{d_v} = \int_0^{\varepsilon_0} \sigma_{ij} \mathrm{d}\varepsilon_{ij} \tag{1}$$

where d_w/d_v is the strain-energy density; σ_{ij} is the stress; ε_{ij} is the strain component; ε_0 is the critical strain corresponding to the maximum stress.

According to the pressure and mid-span deflection curve obtained from tests, the tensile strength, tensile strain and tensile modulus can be calculated by the following equations:

$$R_B = \frac{3LP_B}{2bh^2} \tag{2}$$

$$\varepsilon_B = \frac{6hd}{L^2} \tag{3}$$

$$S_B = \frac{R_B}{\varepsilon_B} \tag{4}$$

where R_B is the tensile strength, MPa; b is the width of the cross section of the specimen, mm; h is the height of

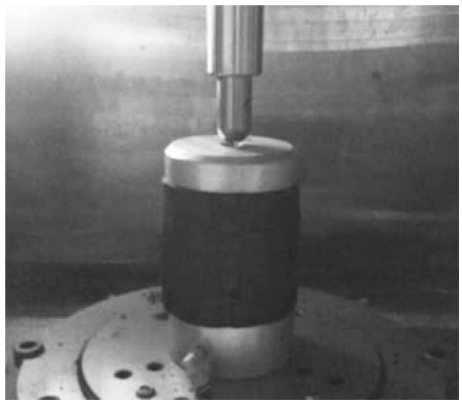

(a)

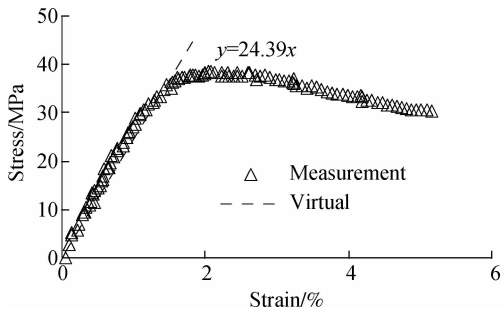

(b)

Fig. 1 Laboratory test of asphalt mortar. (a) Uniaxial compression test; (b) Testing data and fitting curve of asphalt mortar

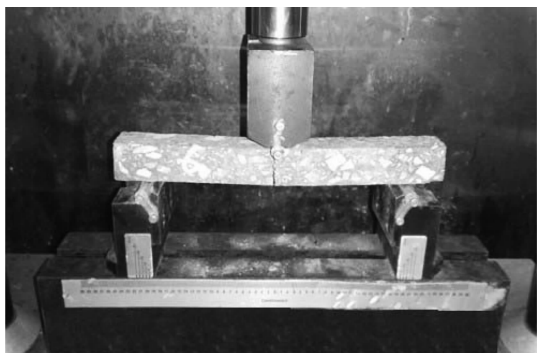

Fig. 2 Bending fracture test

the cross section, mm; L is the span of specimen, mm; P_B is the failure load, N; ε_B is the maximum tensile strain; d is the mid-span deflection when the beam breaks, mm; S_B is the fracture tensile modulus, MPa.

Based on the bending fracture tests of asphalt concrete and asphalt mortar, the tensile strength of asphalt mortar is 5.6 MPa, and the tensile stress-strain curve is obtained from the test data, as shown in Fig. 1. The tensile strength, tensile strain, strain-energy density and tensile modulus are presented in Tab. 3.

Tab. 3 Test data of asphalt concrete

Tensile strength/MPa	Tensile strain/10^{-3}	Strain-energy density/kPa	Tensile modulus/MPa
11.43	2.36	13.51	4 839

2 Modeling of the Virtual Bending Test

2.1 Three-dimensional modeling of asphalt mixture

The virtual sample of asphalt mixture is regarded as a three-phase structure including irregular coarse aggregates, asphalt mortar and air voids. However, the software PFC3D cannot generate irregular aggregates directly; thus, the coarse aggregate sphere units are generated in the virtual space in advance, and the number of sphere units is determined by the volume fraction of aggregates. After that, the "solve" command is used to ensure aggregate sphere units do not overlap, and the graded aggregates sphere units are shown in Fig. 3.

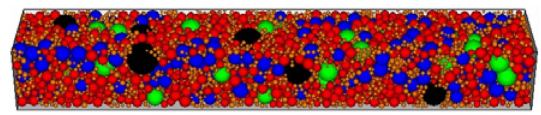

Fig. 3 Generation of aggregate sphere units with gradation

The shape of aggregate used in asphalt pavement is generally irregular convex polyhedron, which has an important effect on the mechanical behavior of the asphalt mixture[15-17]. Thus, in order to make virtual aggregates close to the real shape, geometric information is extracted as the initial parameter for generating polyhedron aggregates. The irregular polyhedron of aggregates is selected from the virtual coarse aggregates library[18], as shown in Fig. 4, and then irregular aggregate generation program is loaded to generate irregular aggregate clumps with grading feature in the virtual specimen space, as shown in Fig. 5. Uniform-sized discrete sphere elements are filled in the remaining space and considered to be asphalt mortar units. Thus, the three-dimensional virtual specimen generated without air voids is finished, as shown in Fig. 6. After traversing discrete elements generated in the virtual specimen, a specific algorithm is used to delete a certain number of asphalt mortar units as a void structure. The cross section from the specimen is used to observe the void structure, as shown in Fig. 7.

In the discretized simulation of asphalt mixture, there are several micro mechanical models used to represent the interaction between contacted particles. The contact stiffness

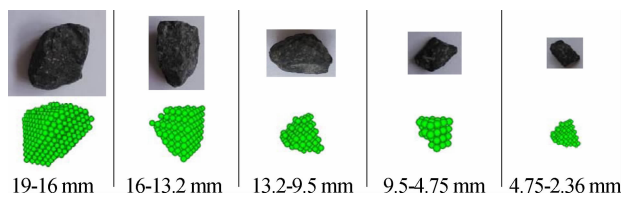

Fig. 4 Selection of irregular aggregates shape

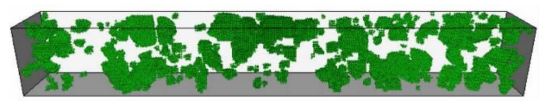

Fig. 5 Generation of irregular aggregates with grading feature

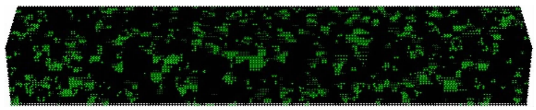

Fig. 6 Generation of virtual specimen without air voids

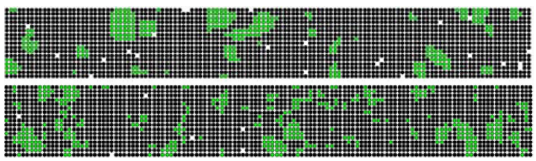

Fig. 7 Observation of air voids from two cross sections

model and the slip model are used to describe the contact between the aggregate particles in simulation. The macro elastic modulus of the aggregate of 55.5 GPa and Poisson's ratio of 0.25 are used to calculate the normal and tangential stiffness of aggregate units by the following equations:

$$k_{\mathrm{n}}=\frac{4\bar{R}^2E_{\mathrm{c}}}{L},\quad k_{\mathrm{s}}=\frac{k_{\mathrm{n}}}{2(1+v)},\quad k_{\varepsilon}=\frac{k_{\varepsilon}^{\mathrm{A}}k_{\varepsilon}^{\mathrm{B}}}{k_{\varepsilon}^{\mathrm{A}}+k_{\varepsilon}^{\mathrm{B}}} \tag{5}$$

where $k_{\varepsilon}^{\mathrm{A}}$ and $k_{\varepsilon}^{\mathrm{B}}$ are the stiffness in the direction of ε for two contact balls, respectively; k_{n} and k_{s} are the normal and tangential contact stiffness between particles with the same property; k_{ε} is the contact stiffness between asphalt mortar and aggregate particles; E_{c} is the macro elastic modulus obtained from the uniaxial compression test.

The normal stiffness and tangential stiffness of aggregate units are 2.22×10^{8} and 8.88×10^{7} N/m, respectively. To simplify the calculation, without regard to the internal fracture in a single aggregate clump during the beam bending fracture process, the tensile strength between the internal units in a single aggregate is set to be a large value, and the friction coefficient between aggregates is set to be 0.5.

As asphalt mixture is close to the linear elastic material at a low temperature, the bonding model and the contact stiffness model are used to describe the contact within asphalt mortar internal units and contact between asphalt mortar and aggregates. The transforming relationship between macro-parameters and meso-parameters are expressed as

$$\bar{R}=\frac{R^{\mathrm{A}}+R^{\mathrm{B}}}{2},\quad \varphi_{\mathrm{n}}=4\bar{R}^2\sigma_{\mathrm{c}},\quad \varphi_{\mathrm{s}}=4\bar{R}^2\tau_{\mathrm{c}} \tag{6}$$

where R^{A} and R^{B} are the radius for two contact balls, respectively, which are both 1 mm in this study; $\bar{R}$ is the average radius between two contacted balls; σ_{c} and τ_{c} are the maximum tensile and shear strength obtained from laboratory fracture tests; ϕ_{n} and ϕ_{s} are the maximum normal and tangential contact force from the contact bonding model.

Based on laboratory tests, the basic input parameters of the bending fracture test calculated by Eqs. (5) and (6) are shown in Tab. 4.

Tab. 4 Input parameters of virtual test

Parameters	Within asphalt mortar	Between asphalt mortar and aggregate	Within aggregates	Between aggregates
φ_{n}/N	22.4	22.4		
φ_{s}/N	8.96	8.96		
$k_{\mathrm{n}}/(\mathrm{N\cdot m^{-1}})$	4.88×10^{6}	9.55×10^{6}	2.22×10^{8}	2.22×10^{8}
$k_{\mathrm{s}}/(\mathrm{N\cdot m^{-1}})$	1.96×10^{6}	3.83×10^{6}	8.88×10^{7}	8.88×10^{7}
μ				0.5

2.2 Validation of virtual bending test

After inputting basic mechanical parameters into the virtual specimen, the load is applied to the specimen to observe the variation of particle displacement (light gray color), contact bond (black mesh) and contact force between particles from the load initiation stage to the crack penetration stage, as shown in Fig. 8. The red color represents tensile contact force between units and the black color represents compressive contact force between units. In the initiation stage, tensile force appears in the region near the both ends of the indenter. The contact tension spread to the bottom with time and increases gradually to the maximum point, then the contact force in the bottom mid-span region begins to dissipate, which is equivalent to the state of crack initiation. After this, the test is entering

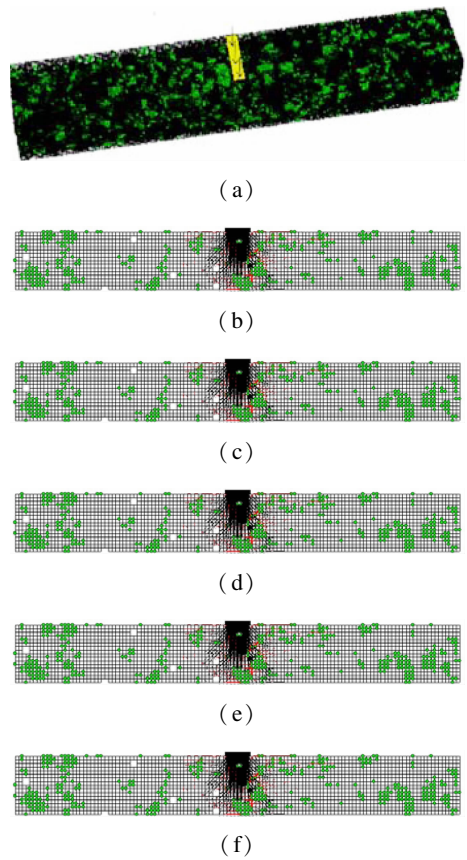

Fig. 8 Observation of virtual bending fracture test. (a) Load condition of the virtual bending test; (b) Initial loading stage; (c) Indenter pressure reaches the maximal value; (d) Initial cracking; (e) Crack extension stage; (f) Crack through stage

into the crack propagation stage. With the mid-span deflection continuing to increase, the contact force near the mid-span region gradually decreases to zero, which is regarded as crack penetration. It can be seen from the virtual bending test that the development process of the fracture at different stages can be clearly captured and visualized, which is the advantage of the virtual test.

After filtering out the initial loading stage, in which the indenter is not touching the specimen, the load-deflection curve of the virtual test can be obtained. The comparison between laboratory test and simulation is shown in Fig. 9. It can be seen that the virtual test curve is similar to the experimental curve, which verifies the validity of the virtual bending test.

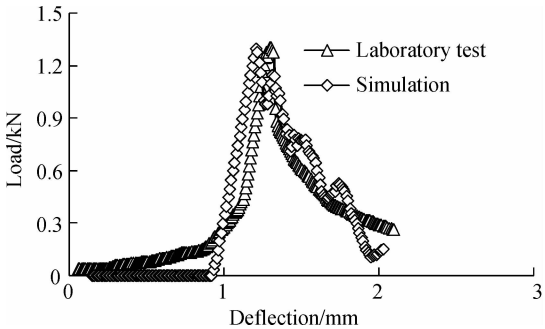

Fig. 9 Test results between the simulation and laboratory test

3 Results and Discussion

3.1 Orthogonal test design

Based on the simulation of virtual fracture test, comparative virtual tests are used to estimate the impacts of meso-scale factors on cracking resistance performance. As shown in Tab. 5, the anti-cracking performance of asphalt mixture is usually studied from three aspects: material composition, mechanical properties and distribution. After comparing the macro factors, seven meso factors are listed in Tab. 5. If each of them takes three levels to do comparison, there will be 2 187 test combinations for comparison, which will be impossible to perform. Therefore, in order to select representative tests to analyze the influence of meso-scale factors on fracture tests, the orthogonal table is used to design comparative tests.

As shown in Tab. 6, 18 groups of virtual bending tests are arranged according to the combination of these factors and levels. The results of stress-strain curves are used to obtain the tensile strength, tensile strain, strain energy density (SED) of the mixture specimen, and results obtained from 18 virtual tests are analyzed by the intuitive analysis method. We can find out the primary and secondary order of factors influencing the bending fracture performance and optimize the test level of each factor.

Tab. 5 Fracture-related factors of asphalt mixture

Volume fraction of coarse aggregates/%	Volume fraction of air voids/%	Normal stiffness of aggregates/(N·m^{-1})	Normal stiffness of asphalt mortar/(N·m^{-1})	Bond strength of asphalt mortar	Horizontal distribution of aggregate	Horizontal distribution of voids
50	12	5.55×10^{7}	1.22×10^{6}	11.2	3∶1∶3	1∶3∶1
55	8	1.11×10^{8}	2.44×10^{6}	22.4	1∶1∶1	1∶1∶1
60	4	2.22×10^{8}	4.88×10^{6}	44.8	1∶3∶1	3∶1∶3

Tab. 6 Orthogonal design

Test No.	Volume fraction/%		Normal Stiffness/(N·m^{-1})		Bond strength/N	Horizontal distribution	
	Coarse aggregates	Voids	Coarse aggregates	Asphalt mortar	Asphalt mortar	Coarse aggregates	Voids
1	50	12	5.55×10^{7}	1.22×10^{6}	11.2	3∶1∶3	1∶3∶1
2	50	8	1.11×10^{8}	2.44×10^{6}	22.4	1∶1∶1	1∶1∶1
3	50	4	2.22×10^{8}	4.88×10^{6}	44.8	1∶3∶1	3∶1∶3
4	55	12	5.55×10^{7}	2.44×10^{6}	22.4	1∶3∶1	3∶1∶3
5	55	8	1.11×10^{8}	4.88×10^{6}	44.8	3∶1∶3	1∶3∶1
6	55	4	2.22×10^{8}	1.22×10^{6}	11.2	1∶1∶1	1∶1∶1
7	60	12	1.11×10^{8}	1.22×10^{6}	44.8	1∶1∶1	3∶1∶3
8	60	8	2.22×10^{8}	2.44×10^{6}	11.2	1∶3∶1	1∶3∶1
9	60	4	5.55×10^{7}	4.88×10^{6}	22.4	3∶1∶3	1∶1∶1
10	50	12	2.22×10^{8}	4.88×10^{6}	22.4	1∶1∶1	1∶3∶1
11	50	8	5.55×10^{7}	1.22×10^{6}	44.8	1∶3∶1	1∶1∶1
12	50	4	1.11×10^{8}	2.44×10^{6}	11.2	3∶1∶3	3∶1∶3
13	55	12	1.11×10^{8}	4.88×10^{6}	11.2	1∶3∶1	1∶1∶1
14	55	8	2.22×10^{8}	1.22×10^{6}	22.4	3∶1∶3	3∶1∶3
15	55	4	5.55×10^{7}	2.44×10^{6}	44.8	1∶1∶1	1∶3∶1
16	60	12	2.22×10^{8}	2.44×10^{6}	44.8	3∶1∶3	1∶1∶1
17	60	8	5.55×10^{7}	4.88×10^{6}	11.2	1∶1∶1	3∶1∶3
18	60	4	1.11×10^{8}	1.22×10^{6}	22.4	1∶3∶1	1∶3∶1

3.2 Analysis of orthogonal test results

Considering that the calculation of the three-dimensional virtual specimen is time-consuming, a two-dimensional slice is used to perform all the tests during the influencing factor analysis. The results of the orthogonal test are presented in Tab. 7. Here, VFC is the abbreviation for volume fraction of coarse aggregates; VFV represents the volume fraction of voids; NSC represents the normal stiffness of coarse aggregates; NSA represents the normal stiffness of asphalt mortar; BSA represents the bond strength of asphalt mortar, HDC represents the horizontal distribution of coarse aggregate and HDV represents the horizontal distribution of air voids, respectively.

Tab. 7 Analysis of orthogonal test results

Test condition	Average tensile strength/MPa		Average tensile strain		Strain energy density/kPa	
	Mean	Range	Mean	Range	Mean	Range
VFC = 50%	12. 33		3 333		20. 73	
VFC = 55%	13. 05	1. 86	2 825	729	18. 46	2. 27
VFC = 60%	14. 19		2 604		18. 50	
VFV = 12%	13. 13		2 708		17. 73	
VFV = 8%	12. 79	0. 86	2 917	429	18. 64	3. 58
VFV = 4%	13. 65		3 137		21. 31	
NSC = 5. 55 × 10^7 N/m	13. 18		2 899		19. 11	
NSC = 1. 11 × 10^8 N/m	13. 08	0. 23	2 900	63	18. 31	1. 39
NSC = 2. 22 × 10^8 N/m	13. 31		2 962		19. 71	
NSA = 1. 22 × 10^6 N/m	12. 87		2 837		18. 25	
NSA = 2. 44 × 10^6 N/m	13. 15	0. 69	2 927	161	19. 15	2. 04
NSA = 4. 88 × 10^6 N/m	13. 56		2 998		20. 29	
BSA = 11. 2 N	12. 11		2 763		16. 75	
BSA = 22. 4 N	13. 25	2. 11	2 829	406	18. 63	5. 55
BSA = 44. 8 N	14. 21		3 169		22. 30	
HDC = 3∶1∶3	13. 80		2 812		19. 33	
HDC = 1∶1∶1	12. 94	0. 97	2 854	284	18. 39	1. 57
HDC = 1∶3∶1	12. 83		3 096		19. 96	
HDV = 1∶3∶1	12. 84		2 792		17. 98	
HDV = 1∶1∶1	13. 57	0. 73	2 937	242	19. 76	1. 97
HDV = 3∶1∶3	13. 16		3 033		19. 94	

In view of the orthogonal analysis, statistical software SPSS is adopted to calculate the value of average tensile strength, average tensile strain, strain energy density and the range from different test levels, respectively. According to the range value shown in Fig. 10(a), the factors influencing the value of tensile strength are listed in decreasing order as follows: BSA > VFC > HDC > VFV > HDV > NSA > NSC. So, the maximum tensile strength is obtained when the combination is as follows: BSA = 44. 8 N, VFC = 60%, HDC = 3∶1∶3, VFV = 4%, HDV = 1∶1∶1, NSA = 4. 88 × 10^6 N/m, NSC = 2. 22 × 10^8 N/m. The bond strength of asphalt mortar is found to be the most important determinant of tensile strength, while three levels of six other factors cannot be overlooked in the analysis. Similarly, according to the range value shown in Fig. 10(b), the factors influencing the value of tensile strain are listed in decreasing order as follows: VFC > VFV > BSA > HDC > HDV > NSA > NSC. The maximum tensile strain can be obtained when the combination is as follows: VFC = 50%, VFV = 4%, BSA = 44. 8 N, HDC = 1∶3∶1, HDV = 3∶1∶3, NSA = 4. 88 × 10^6 N/m, NSC = 2. 22 × 10^8 N/m, and the volume fraction of coarse aggregates is found to be the most important determinant of the tensile strain. The strain-energy density is regarded as a comprehensive index of the fracture performance of asphalt concrete. According to the

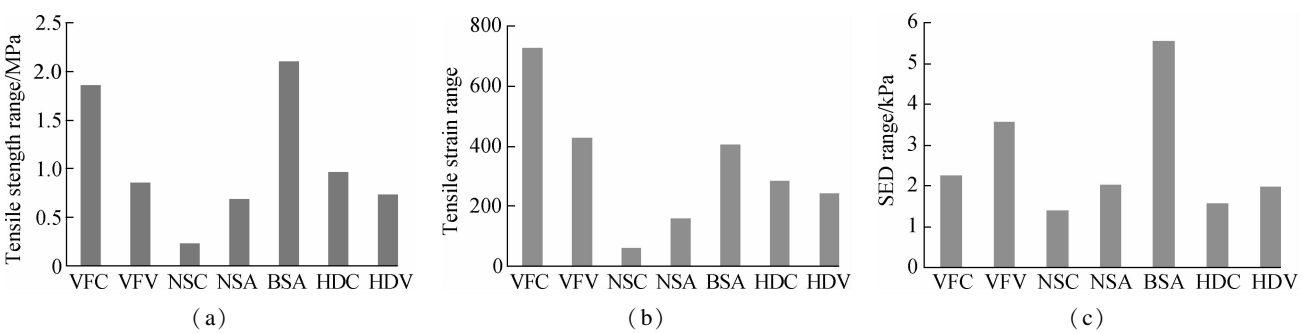

Fig. 10 Orthogonal test results. (a) Range chart of tensile strength; (b) Range chart of tensile strain; (c) Range chart of strain energy density

range value shown in Fig. 10(c), the factors influencing the value of strain-energy density are listed in decreasing order as follows: BSA > VFV > VFC > NSA > HDV > HDC > NSC. The maximum value is obtained when the combination is as follows: BSA = 44.8 N, VFV = 4%, VFC = 50%, NSA = 4.88×10^6 N/m, HDV = 3∶1∶3, HDC = 1∶3∶1, NSC = 2.22×10^8 N/m, the value of the bond strength of asphalt mortar is found to be the most important determinant of the strain-energy density.

4 Conclusions

1) Based on the random generation algorithm, the three-dimensional microstructure of asphalt concrete can be built for the virtual bending test. Suitable micro mechanical contact models can be applied to the virtual specimen. The virtual bending fracture test can be performed well by the PFC3D with three heterogeneous features.

2) The development process of crack failure is clearly captured and visualized at every stage. The load-deflection curve of virtual test matches the experimental curve, indicating that the virtual test can be validated by the laboratory fracture test.

3) The orthogonal test is applied to analyze the impacts of seven meso-scale factors on fracture performance. The factors influencing the value of tensile strength, tensile strain and strain-energy density are listed in decreasing order as follows: BSA > VFC > HDC > VFV > HDV > NSA > NSC, VFC > VFV > BSA > HDC > HDV > NSA > NSC and BSA > VFV > VFC > NSA > HDV > HDC > NSC, respectively.

4) Based on the range value and variance analysis, the value of the bond strength of asphalt mortar is found to be the most important determinant of tensile strength. The volume fraction of coarse aggregates is considered to be the most important determinant of tensile strain, while the value of the bond strength of asphalt mortar is found to be the most important determinant of strain-energy density.

References

[1] Kim K W, El Hussein M. Variation of fracture toughness of asphalt concrete under low temperatures[J]. *Construction and Building Materials*, 1997, **11**(7): 403 - 411. DOI:10.1016/s0950-0618(97)00030-5.

[2] Li X, Marasteanu M. The fracture process zone in asphalt mixture at low temperature[J]. *Engineering Fracture Mechanics*, 2010, **77**(7): 1175 - 1190. DOI: 10.1016/j.engfracmech.2010.02.018.

[3] Yang J, Jiao L, Wang K, et al. Three dimensional simulation of virtual triaxial shear test for asphalt mixture based on discrete element method[J]. *Journal of Southeast University (Natural Science Edition)*, 2014, **44**(5): 1057 - 1061. DOI: 10.3969/j.issn.1001-0505.2014.05.032. (in Chinese)

[4] Liu Q, Cao D. Research on material composition and performance of porous asphalt pavement[J]. *Journal of Materials in Civil Engineering*. 2009, **21**(4): 135 - 140. DOI: 10.1061/(asce)0899-1561(2009)21:4(135).

[5] Jiang X, Qian Z, Song X. Experimental study on virtual fracture of epoxy asphalt concrete based on discrete element method[J]. *Journal of Southeast University (Natural Science Edition)*, 2014, **44**(1): 173 - 177. DOI: 10.3969/j.issn.1001-0505.2014.01.031. (in Chinese)

[6] Wagoner M, Buttlar W, Paulino G, et al. Development of a single-edge notched beam test for asphalt concrete mixtures[J]. *Journal of Testing and Evaluation*, 2005, **33**(6): 452 - 460. DOI:10.1520/jte12579.

[7] Wagnoner M P, Buttlar W G, Paulino G H. Disk-shaped compact tension test for asphalt concrete fracture[J]. *Experimental Mechanics*, 2005, **45**(3): 270 - 277. DOI: 10.1007/bf02427951.

[8] Kim H, Wagoner M P, Buttlar W G. Simulation of fracture behavior in asphalt concrete using a heterogeneous cohesive zone discrete element model[J]. *Journal of Materials in Civil Engineering*, 2008, **20**(8): 552 - 563. DOI:10.1061/(asce)0899-1561(2008)20:8(552).

[9] Kim H, Buttlar W G. Discrete fracture modeling of asphalt concrete[J]. *International Journal of Solids and Structures*, 2009, **46**(13): 2593 - 2604. DOI:10.1016/j.ijsolstr.2009.02.006.

[10] Chen J, Pan T, Huang X. Discrete element modeling of asphalt concrete cracking using a user-defined three-dimensional micromechanical approach[J]. *Journal of Wuhan University of Technology-Mater Sci Ed*, 2011, **26**(6): 1215 - 1221. DOI:10.1007/s11595-011-0393-z.

[11] Mahmoud E, Masad E, Nazarian S. Discrete element analysis of the influences of aggregate properties and internal structure on fracture in asphalt mixtures[J]. *Journal of Materials in Civil Engineering*, 2010, **22**(1): 10 - 20. DOI:10.1061/(asce)mt.1943 - 5533.0000005.

[12] Wang J, Qian Z, Wang L. Three-dimensional fracture modeling of epoxy asphalt concrete using a heterogeneous iscrete element model [C]//*Transportation Research Board 92nd Annual Meeting*. Washington, DC, USA, 2013:13-2994.

[13] Eckwright F, Jung S J, Abdo A M A. Utilizing a particle flow code in 2 dimensional discrete element method of fracture resistance evaluation of HMA and brittle rock [J]. *Asian Journal of Civil Engineering*, 2014, **15**(1):9 - 21.

[14] Yang X, Dai Q, You Z, et al. Integrated experimental-numerical approach for estimating asphalt mixture induction healing level through discrete element modeling of a single-edge notched beam test[J]. *Journal of Materials in Civil Engineering*, 2015, **27**(9): 04014259. DOI: 10.1061/(asce)mt.1943 - 5533.0001231.

[15] Chen J, Wang L B, Huang X M. Micromechanical modeling of asphalt concrete fracture using a user-defined three-dimensional discrete element method [J]. *Journal of Central South University*, 2012, **19**(12): 3595 - 3602. DOI:10.1007/s11771-012-1447-x.

[16] Kwan A K H, Mora C F. Effects of various shape parameters on packing of aggregate particles[J]. *Magazine of Concrete Research*, 2001, **53**(2): 91 - 100. DOI: 10.1680/macr.2001.53.2.91.

[17] Rocco C G, Elices M. Effect of aggregate shape on the mechanical properties of a simple concrete[J]. *Engineering Fracture Mechanics*, 2009, **76**(2): 286 - 298. DOI: 10.1016/j.engfracmech.2008.10.010.
[18] Jin C, Yang X, You Z. Automated real aggregate modelling approach in discrete element method based on X-ray computed tomography images[J]. *International Journal of Pavement Engineering*, 2015, **18**(9): 837 - 850. DOI:10.1080/10298436.2015.1066006.

细观因素对密级配沥青混合料低温断裂试验的影响仿真模拟研究

张 垚[1] 黄晓明[1] 马 涛[1] 张德育[2]

([1] 东南大学交通学院, 南京 210096)
([2] 南京工程学院建筑工程学院, 南京 211167)

摘要: 为了研究关键因素对密级配沥青混凝土低温断裂性能的影响,采用离散单元法(DEM)和三维颗粒流程序 PFC3D 模拟弯曲断裂试验. 基于随机生成算法和虚拟不规则粗集料库模拟集料级配和不规则形状、沥青砂浆以及空隙率的生成过程. 然后,在虚拟试件中添加细观力学接触本构模型进行虚拟断裂试验,虚拟试验结果与室内试验结果对比验证了虚拟试验结果的有效性. 此外,基于虚拟仿真采用正交试验研究集料和空隙的体积分数、集料和沥青砂浆的刚度、沥青砂浆内部粘结强度以及集料和空隙的分布对虚拟断裂试验的影响. 研究表明,上述因素对断裂性能都有不同程度的影响,其中对弯拉强度和弯曲应变能密度影响最大的是沥青砂浆的粘结强度,对弯拉应变影响最大的是粗集料的体积分数. 为了得到较好的密级配沥青混合料低温断裂性能,考虑沥青砂浆和集料的细观结构非常重要.

关键词: 沥青混合料; 断裂性能; 低温; 虚拟试验; PFC3D; 影响因素
中图分类号: TU414